Hydration Energies of Sodiated Amino Acids from Gas-Phase Equilibria Determinations

Henryk Wincel†

Institute of Physical Chemistry, Polish Academy of Sciences, 01-224 Warsaw, Poland

Received: March 18, 2007; In Final Form: April 19, 2007

The sequential hydration of a number of sodiated amino acids is investigated using a high-pressure mass spectrometer. Ions produced continuously by electrospray are injected into the reaction chamber in the pulsed mode where the hydration equilibria, $AANa^+(H_2O)_{n-1} + H_2O = AANa^+(H_2O)_n$ (AA = Val, Pro, Met, Phe, and Gln), and the temperature dependence of the equilibrium constants are measured in the gas phase at 10 mbar (N_2 bath gas and known pressure of H_2O). The thermochemical properties, ΔH_n°, ΔS_n°, and ΔG_n°, for the hydrated systems are determined and discussed in conjunction with the structural forms. The results show that the binding energies of water to the $AANa^+$ complexes decrease with the increasing number of water molecules. The present results from equilibrium measurements are compared to those from earlier studies obtained by other techniques. A correlation between the free energy changes for the addition of the first and second water molecules to $AANa^+$, and the corresponding sodium ion affinities, is observed. Generally, the hydration free energy becomes weaker as the AA-Na^+ bond strength increases.

Introduction

Water is known to play a critical role in biological systems. Alkali metal ions, such as Na^+ and K^+, also play very important roles in the biophysical processes of living systems.[1] For example, they participate in activation of enzyme functions, maintaining osmotic equilibrium in cells, in transport of cations across membrane channels, biological signaling in the nervous systems,[1−3] etc. In this context, a number of experimental and theoretical studies have been performed on alkali metal ion/amino acid complexes.[4−19] These investigations indicate that in the absence of a solvent, most of the sodiated amino acids exist in the charge solvated (CS) form, in which the metal cation binds to the amino nitrogen and carbonyl oxygen (NO coordination). In the proline−Na^+ lowest-energy complex, the cation is bound between the O atoms of the zwitterionic form (OO coordination).[13,18] Several studies[8,9,15,16,19] have established that interactions with the side chain of the amino acids are also important to the binding of Na^+ in some cases.

In extensive studies of the dissociation rates and water binding energies of Val·$M^+(H_2O)_{n=1-6}$, (M = Li, Na, and K), using blackbody infrared radiation dissociation (BIRD) along with computational modeling, Williams and co-workers[20] showed that two water molecules change the binding position of Na^+ to valine from (NO) to (OO) coordination. In the case of a lithiated complex, three water molecules change Li^+ binding from (NO) to (OO) coordination.[21] Very recently, infrared spectroscopy studies on Val·$Li^+(H_2O)_{n=1-4}$ and Val·$H^+(H_2O)_{n=1-4}$ by Kamariotis et al.[22] provided support for the change in Li^+ location upon addition of the third water molecule, but in contrast to the BIRD experiments,[21] no evidence for zwitterion formation with the addition of up to four water molecules has been found. Williams and co-workers[23,24] also investigated the water binding energies for $GlnLi^+(H_2O)_{n=1-2}$ and $GlnNa^+(H_2O)_{n=1-2}$, and found that Gln is nonzwitterionic in these complexes. They recently investigated[25] the structures of lithiated and sodiated α-methyl-proline and determined the first water binding energies to these complexes. Armentrout et al. used threshold collision-induced dissociation (TCID) experiments together with calculations to study the structures of $GlyNa^+(H_2O)_{n=1-4}$[26] and $ProNa^+(H_2O)_{n=1-4}$,[27] and the sequential bond energies of water to the $GlyNa^+(H_2O)_{n=0-3}$ and $ProNa^+(H_2O)_{n=0-3}$ systems.

Thermodynamic information on interactions between cationized amino acids and individual water molecules is of great interest for a better understanding of biomolecular processes in living systems. Gas-phase studies of sequential addition of water molecules to protonated and cationized amino acids can provide information on the specific interaction of small numbers of solvent molecules that is not available from solution studies.

We have previously described an ion source designed to determine of the thermochemical properties of gas-phase sequential hydration for biomolecule ions under high-pressure equilibrium conditions.[28] This source was employed to study the enthalpy and entropy changes associated with hydration of protonated alkylamines, amino acids and dipeptides. As a continuation of that study, here we report on the hydration energetics for a number of sodiated amino acids, $AANa^+$ (AA = Val, Pro, Met, Phe, and Gln), produced by electrospray.

Experimental

All experiments were performed with a high-pressure mass spectrometer (HPMS) using the homemade electrospray ionization (ESI) source, which has been previously described in detail.[28] A schematic diagram of the source is shown in Figure 1. Briefly, sodiated amino acids were obtained by electrospray from solutions containing 2.0 mM AA and 2.0 mM NaOH in methanol. The electrospray emitter, ESC, was produced from a fused-silica capillary (15 μm i.d., 150 μm o.d.) inserted into a stainless steel capillary. To provide electrical contact, the emitter end (∼10 mm) was coated with a conductive polyimide/graphite mixture. The sample was supplied to the

† Tel: +48 22 343-3253. Fax: +48 22 632-52-76. E-mail: wincel@ichf.edu.pl.

10.1021/jp0721595 CCC: $37.00
Published on Web 06/09/2007

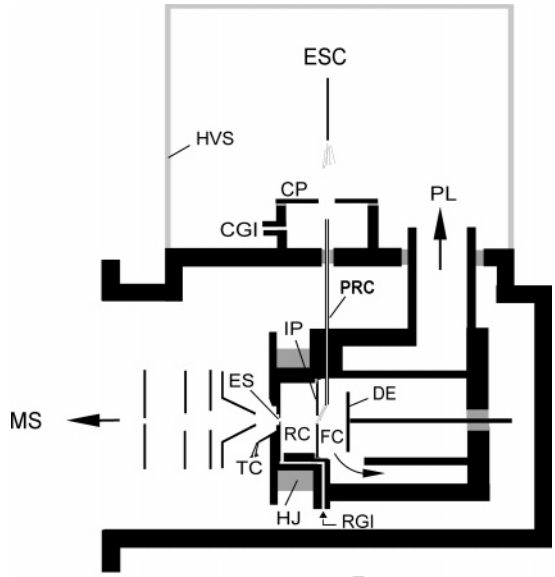

Figure 1. Scheme of the combined electrospray emitter and high-pressure ion source with pulsed ion beam: (ESC) electrospray capillary; (HVS) high-voltage shield; (CP) curtain plate; (CGI) curtain gas inlet; (PL) pumping lead; (PRC) pressure reducing capillary; (FC) forechamber; (DE) deflection electrode; (IP) interface plate; (RC) reaction chamber; (RGI) reaction gas inlet; (TC) thermocouple; (ES) ion exit slit; (HJ) electrically heated jacket.

electrospray needle by a syringe pump (Ascor apparatus, Model 11a) from a glass syringe (0.5 mL Hamilton) at a rate of 0.8 μL/min.

After formation, the clustered ionic complexes are desolvated by a counter current flow of heated nitrogen (~90 °C) supplied through curtain gas inlet, CGI, and in a heated (~100 °C) pressure reducing capillary, PRC, through which they are transported into the forechamber, FC, and then deflected toward a 3-mm orifice in the interface plate, IP, leading to the reaction chamber, RC, (7 mm length; 20 mm i.d.). The ions drift through the RC toward the exit slit, ES, (15 μm × 3 mm) under the influence of a weak potential applied to the IP (2V/cm at 10 mbar). The ions drifting across the RC are hydrated and reach equilibrium prior to being sampled to the mass analysis section of the mass spectrometer. Ions leaving the RC are analyzed by a magnetic mass spectrometer. Ion detection was provided by a secondary electron scintillation detector of the Daly type with an aluminum conversion dynode using a short rise-time photomultiplier (Hamamatsu R-647−04). The output pulses of the multiplier were counted using a multichannel scaler with dwell time per channel of 1 μs.

Two types of experiments were carried out with this ion source: mass spectra were registered with continuous ion sampling, while for the hydration equilibria measurements, narrow "slices" of the continuous ion beam were injected into the RC in a pulsing mode. The latter mode of operation allows for measurements of the arrival time distribution (ATD) of ions moving across the RC. Typical potentials used with the continuous ion beam were as follows: ESI emitter, approximately 4 kV; PRC and RC, 2 kV; electrode DE, 2050 V; electrode IP, 2016 V. In the pulsing mode of operation, $V_{IP} = V_{DE} = 2014$ V and an injection pulse (+34 V; 60 μs; rise time 10 ns) was applied to the electrode DE with repetition of 1 ms. The pulsing sequence was performed several thousand times to accumulate enough ion counts in time channels for a given mass.

The reagent gas mixture consisting of pure N_2 as the carrier gas at about 10 mbar and a known partial pressure of water

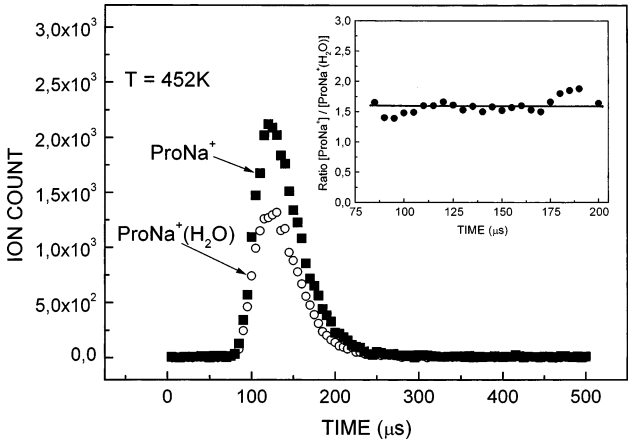

Figure 2. Arrival time distributions of the reactant, $ProNa^+$, and product, $ProNa^+(H_2O)$, ions. The inset shows the ion intensities ratio of $[ProNa^+/ProNa^+(H_2O)]$ as a function of ion residence time.

vapor (0.02−0.20 mbar) was supplied to the RC via the reactant gas inlet (RGI) at a flow rate of ~100 mL/min. The pressure was measured with an MKS capacitance manometer attached near the inlet of the RGI. Water was introduced into the heated N_2 bath gas flow line with a syringe pump. The amount of water injected into the nitrogen gas flow was kept constant throughout the temperature dependent measurements of the equilibrium constants. Water concentrations were controlled continuously with a calibrated temperature and humidity transmitter (Delta OHM, Type DO 9861T, Italy) inserted into the carrier gas flow line. The RC temperature was monitored by an iron−constantan thermocouple which was embedded close to the ion exit slit (see Figure 1); the temperature can be varied from ambient to 300 °C by electrical heaters.

Chemicals. Amino acids (Val, Met, Pro, Phe and Gln) were obtained from Aldrich Chemical Co. NaOH and CH_3OH were purchased from Chempur (Poland). Water was deionized with a Millipore purifier, type Elix 5 (Austria).

Results

The energies of hydration of sodiated AA were obtained from the determination of the gas-phase equilibria represented by the following general reaction:

$$AANa^+(H_2O)_{n-1} + H_2O = AANa^+(H_2O)_n \qquad (1)$$

for which the equilibrium constants, $K_{n-1,n}$, for a standard state pressure of 1000 mbar were determined from the expression (2):

$$K_{n-1,n} = (I_n\, 1000/I_{n-1}\, P) \qquad (2)$$

where I_n and I_{n-1} are recorded ATD peak areas of the respective ions and P is the known partial pressure (in mbar) of H_2O in the bath gas. The equilibrium attainment was checked by comparing the ATDs of the reactant and product ions, and their ATDs were to be the same (except for the scaling factor of the peak amplitude). A typical example is shown in Figure 2 for $ProNa^+$ and $ProNa^+(H_2O)$. The inset of the figure shows that within the error limits and the limits of statistical noise, the ratio of $[ProNa^+/ProNa^+(H_2O)]$ remains essentially constant, implying that the system is at equilibrium under the present experimental conditions.

The thermochemical properties, ΔH_n° and ΔS_n°, were derived from temperature dependent measurements of the equilibrium constants using the van't Hoff equation:

$$\ln K_{n-1,n} = (\Delta S_n^\circ/\mathrm{R}) - (\Delta H_n^\circ/\mathrm{RT}) \quad (3)$$

Representative van't Hoff plots for the systems studied here are shown in Figure 3. No bending in the van't Hoff plots was observed in the present experiments. The weighted least-squares fitting procedure was used to obtain the slopes and intercepts of each line. The slopes determine the enthalpy change (ΔH_n°) for the hydration equilibria (eq 1) and the intercepts yield the corresponding ΔS_n° values. The free energy can be obtained at any temperature from $\Delta G_n^\circ = \Delta H_n^\circ - T\Delta H_n^\circ$. The experiments were repeated 2−3 times to determine the standard deviation of the ΔH_n° and ΔS_n° values. The thermochemical data thus obtained are summarized in Table 1, along with literature results. In the case of the $MetNa^+(H_2O)_n$, $PheNa^+(H_2O)_n$ and $GlnNa^+(H_2O)_n$ systems, determination of the binding energies was possible only for $n \leq 2$, because higher hydration steps require equilibration temperatures below room temperature, which are as yet not accessible with the present reaction chamber.

Discussion

As shown in Table 1, for $ValNa^+(H_2O)_{n=1,2}$ and $GlnNa^+(H_2O)$, there is excellent agreement between the present $|\Delta H_1^\circ|$ values, the high-pressure equilibrium results, and the binding energies experimentally derived from the BIRD kinetics studies of refs 20, 23, 24, and 29. The present $|\Delta H_2^\circ|$ value for $GlnNa^+(H_2O)_2$ is a bit higher than that from the BIRD data,[24] but the agreement is within the margin of experimental errors.

For $ProNa^+(H_2O)_{n=1-4}$, the present values of $-\Delta H_n^\circ$ agree reasonably well with the computational results obtained by Armentrout and co-workers,[27] and are also in acceptable agreement with those experimentally determined by these authors for $n = 1$ and 2, while for $n = 3$ and 4 they are in substantial disagreement. Except for $n = 1$, disagreement between the ΔS_n° and ΔG_n° values obtained in the present work and those reported in ref 26 is completely outside experimental uncertainty (Table 1).

In Figure 4a the binding energies (BE's), $-\Delta H_n^\circ$, are plotted as a function of n for the $ValNa^+(H_2O)_n$ and $ProNa^+(H_2O)_n$ systems, together with those reported in the literature for the $Na^+(H_2O)_{n=3-6}$ cluster.[30] The $-\Delta H_n^\circ$ values are seen to decrease with n, indicating that the interaction involved in these clusters is electrostatic in nature. In general, this trend can be attributed to a partial delocalization of the charge on the hydration site(s) over the accommodated water molecules, which results in weaker electrostatic interaction in the subsequent hydration reactions. Moreover, the water binding energy decreases due to the exchange repulsion between the ligand molecules.

The binding energy of the first water molecule to $ValNa^+$ (15.9 kcal/mol) is very close to that of the third (15.8 kcal/mol) water in the $Na^+(H_2O)_n$ cluster.[30] However, the binding energies of the second and third water in $ValNa^+(H_2O)_n$ are weaker (1.3 kcal/mol) than those of the fourth and fifth, respectively, in $Na^+(H_2O)_n$(Figure 4a). Considering that the binding energies of ligand molecules in cluster ions with electrostatic interaction generally decrease monotonically with the growth of the cluster size n, the observed irregular decrease in $-\Delta H_n^\circ$ with $n = 1 \rightarrow 2$ for $ValNa^+(H_2O)_n$ is interesting. This observation might reflect a change in the mode of the metal ion complexation in the reaction $ValNa^+(H_2O)_{1\rightarrow 2}$. Williams and co-workers[20] have demonstrated a change in the sodium ion binding from NO coordination to OO coordination upon the addition of the second water molecule to $ValNa^+(H_2O)$. Similarly, Armentrout et al.[26] found that the addition of the second water molecule to $GlyNa^+$ changes the preferable sodium binding site from NO to C═O coordination where one of the water molecules is attached to the hydroxyl group. Scheme 1 presents a plausible mechanistic scenario for the hydration of sodiated valine, which involves the lowest-energy structures of the $ValNa^+(H_2O)_{n=0-2}$ complexes, based on the calculations.[20,29]

The experimental and theoretical results[20,29] suggest that the water molecule in $ValNa^+(H_2O)$ interacts directly with the NO-coordinated Na^+ ion (Structure **2**), while in the $ValNa^+(H_2O)_2$ complexes the sodium and water molecules are coordinated to the C terminus of valine, but the form of valine in the latter complexes remains unspecified (structure **3a** or **3b**). Calculations[20] indicate that the most stable OO-coordinated nonzwitterionic conformation **3a** is slightly lower in energy (3 kcal/mol) than the zwitterionic form **3b**. However, the barrier for conversion between these structures is expected to be little (2−3 kcal/mol[31,32]), and therefore, the interconversion **3a** ↔ **3b** cannot be excluded within the temperature range examined.

As shown in Table 1, the $-\Delta S_n^\circ$ values for $ValNa^+(H_2O)_n$ with $n = 1-3$ are essentially the same, suggesting that the water molecules interact with the sodiated valine complex without causing serious restriction in the freedom of H_2O motion with the increase of n. This observation is consistent with both OO-coordinated structures, **3a** and **3b**, where the water molecules are attached to different solvation sites. For the $ValNa^+(H_2O)_3$ complex, the calculations[19] predict the most stable structure is formed when the third water molecule interacts solely with the Na^+ ion of a nonzwitterionic form **3a** or hydrates the $-NH_3^+$ group in the conformation **3b**.

As noted above, in the $ValNa^+(H_2O)$ case, the present $-\Delta H_1^\circ$ value is identical to the threshold dissociation energy for loss of water from this complex[29] (Table 1), which was found to have nonzwitterionic structure **2**; for the zwitterionic form, the energetic threshold for the loss of water from the complex should be lower by ∼1 kcal/mol.[28] It is, therefore, reasonable to expect that the structures **1** ↔ **2** are involved in the (0,1) hydration equilibria determinations (eq 1), although we cannot exclude the possibility that some isomerization of **2** to the OO coordinated forms of $ValNa^+(H_2O)$ occurs. For the $ValNa^+(H_2O)$ system, the barriers for isomerization between the lowest energetic structures are not known. Calculations by Marino et al.[13] have shown that the barrier for isomerization between the nonzwitterionic and zwitterionic forms of $AlaNa^+$ is 17 kcal/mol, whereas for $AlaNa^+(H_2O)$ the barrier associated with the displacement of the Na^+ ion and water ligands from NO coordination to OO-coordinated forms (both nonzwitterionic and zwitterionic) of alanine is calculated to be substantially lower (∼14 kcal/mol).[31] It seems likely that the conversion barrier between the NO and OO-coordinated sodium ion structures in $ValNa^+(H_2O)$ is close to that for $AlaNa^+(H_2O)$. If this is the case, the complexation of H_2O and $ValNa^+$ can lead to the formation of a chemically activated (15.9 kcal/mol) adduct, $ValNa^+(H_2O)$, with sufficient internal energy for conversion between these forms prior to the water loss in the reverse (0,1) hydration reaction, eq 1. However, in contrast to the direct loss of a water molecule, this conversion requires overcoming several intermediate steps which are kinetically controlled by the energetic barriers[31] and should be entropically unfavorable. Nevertheless, the experimental and computational results from gas-phase H/D exchange of D_2O with $ValNa^+$ and other sodiated amino acids at 300 K indicate that this process could lead to the isomerization of the $ValNa^+-D_2O$ reaction complex structure from the nonzwitterionic to zwitterionic form.[31] In the

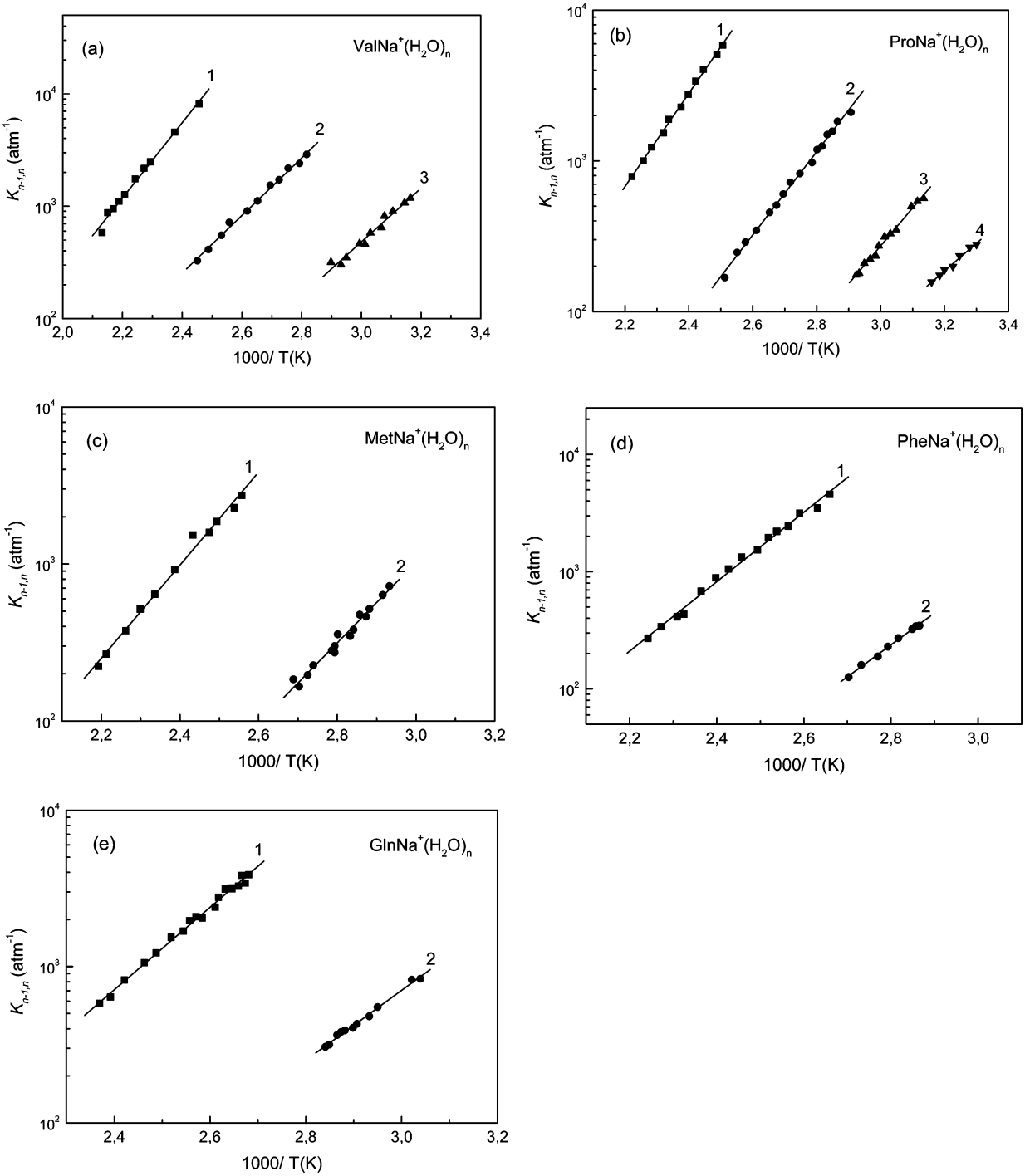

Figure 3. van't Hoff plots of equilibrium constants for the gas-phase reactions $AANa^+(H_2O)_{n-1} + H_2O = AANa^+(H_2O)_n$, where AA equals (a) Val; (b) Pro; (c) Met; (d) Phe; and (e) Gln. The numbers shown in the figures correspond to the value of *n*.

present experiments, no noticeable anomalous van't Hoff plots are observed (Figure 3). This may suggest that the presence of another structure of the $ValNa^+(H_2O)$ complex in the (0,1) equilibrium is minor, if it exists at all. With regard to the (1,2) equilibrium, it seems likely that $ValNa^+(H_2O)$ formed in the reverse reaction from the OO-coordinated complex, $ValNa^+(H_2O)_{2\rightarrow1}$, is still OO-coordinated, because there is insufficient energy to overcome the substantial barrier (~12 kcal/mol,[31]) for back isomerization to the NO-coordinated structure **2**.

For $GlnNa^+(H_2O)_{n=1,2}$, the present $-\Delta H_n^\circ$ values are in good agreement with the experimental and calculated binding energies obtained by Williams and co-workers[23,24] for the nonzwitterionic forms of Gln in these complexes, Table 1. Their results are of special interest in the context of the present experimental data. They predicted that for the $GlnNa^+$ complex, the lowest-energy NOO-coordinated nonzwitterionic form is 1.9 kcal/mol lower in energy than that of the zwitterionic form. Relevant arrangements of some of the most plausible conformations found[23,24] for the hydrated complexes are illustrated in Scheme 2.

The nonzwitterionic structures such as **4** and **5** appear to be the most likely forms of the $GlnNa^+(H_2O)_n$ complexes with $n = 1$ and 2, respectively, as deduced from both BIRD experiments and calculations.[23,24] Although the lowest-energy zwitterionic forms, **4a** and **5a**, of the $GlnNa^+(H_2O)_{n=1,2}$ complexes are more stable by about 0.17 and 3.6 kcal/mol, than

TABLE 1: Experimental ΔH_n°, ΔS_n°, and ΔG_n° Values[a,b] for the Sequential ($n-1 \rightarrow n$) Gas-Phase Hydration of the Sodiated Amino Acids[c]

ion	n	$-\Delta H_n^\circ$ (kcal/mol)	$-\Delta S_n^\circ$ (cal/mol K)[d]	$-\Delta G_n^\circ$ (kcal/mol)[e]	ref
$ValNa^+$	1	15.9 (0.4)	20.9 (0.8)	9.7 (0.6)	
		15.9 (0.2)[f]			29
	2	12.2 (0.4)	18.8 (1.3)	6.7 (0.8)	
		12.5[g]			20
	3	11.0 (0.6)	21.0 (2.0)	4.8 (1.2)	
$ProNa^+$	1	14.5 (0.3)	18.8 (0.6)	8.9 (0.4)	
		15.8 (1.2)[h] *(15.1)*[i]	*22.9 (5.7)*[j]	*9.0 (2.1)*	27
	2	12.9 (0.3)	21.9 (0.8)	6.4 (0.5)	
		11.3 (1.2)[h] *(12.9)*[i]	*33.6 (4.4)*[j]	*1.3 (1.8)*	27
	3	11.6 (0.5)	23.5 (1.2)	4.6 (0.8)	
		7.7 (1.1)[h] *(10.0)*[i]	*31.5 (6.3)*[j]	−1.7 (2.2)	27
	4	8.4 (0.4)	16.6 (1.5)	3.5 (0.9)	
		5.3 (1.6)[h] *(9.1)*[i]	*31.4 (6.3)*[j]	−4.0 (2.4)	27
$MetNa^+$	1	13.7 (0.7)	19.1 (1.8)	8.0 (1.2)	
	2	11.8 (0.5)	21.4 (1.4)	5.4 (0.9)	
$PheNa^+$	1	13.6 (0.3)	19.3 (1.0)	7.9 (0.6)	
	2	12.3 (0.3)	23.6 (1.0)	5.3 (0.8)	
GlnNa	1	12.2 (0.3)	16.0 (0.8)	7.4 (0.5)	
		12.4 (0.2)[k]			23
	2	10.3 (0.4)	17.8 (1.0)	5.0 (0.7)	
		9.6 (0.5)[l]			24

[a] Standard pressure is 1000 mbar. [b] Uncertainties are listed in parentheses. [c] Binding energies (in italics) from the literature are included for comparison. [d] Results given to the temperature of the van't Hoff plot. However, since the ΔS° dependence upon the temperature is small, ΔS° values are approximately equal to those at 298 K. [e] ΔG° at 298 K. [f] Using blackbody infrared radiative dissociation.[29] [g] Binding energy on the measured dissociation kinetics.[20] [h] Using threshold collision-induced dissociation.[27] [i] Calculated at the MP2 (full) level.[27] [j] Calculated at the B3LYP/6-311+G** level. [k] Using blackbody infrared radiative dissociation.[23] [l] Using blackbody infrared radiative dissociation.[24]

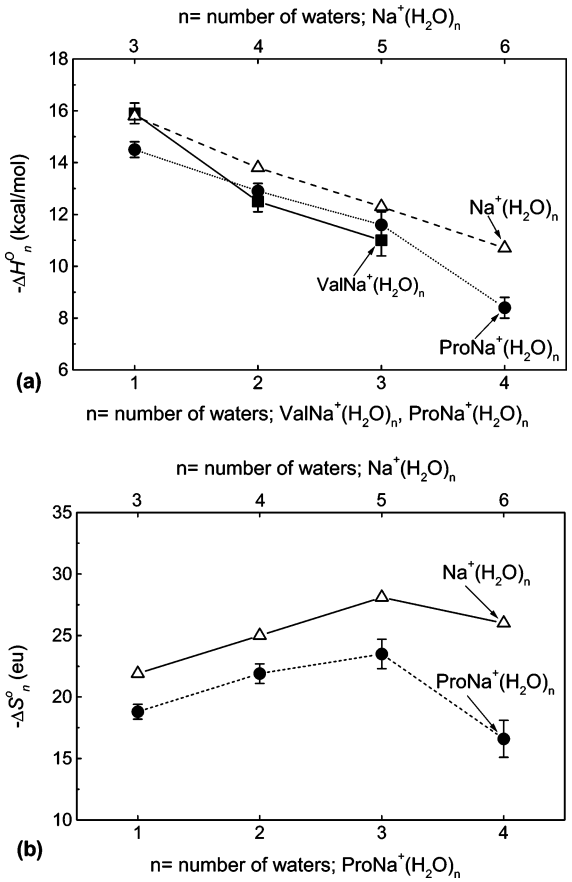

Figure 4. Comparison of the n dependence of: (a) the water binding energies ($-\Delta H_n^\circ$) and (b) entropies of hydration ($-\Delta S_n^\circ$) at 298 K for the indicated complexes. The $-\Delta H_n^\circ$ and $-\Delta S_n^\circ$ values for $Na^+(H_2O)_n$, ref. 30.

the nonzwitterionic ones, **4** and **5**, respectively, no evidence for the isomerization **4** → **4a** and **5** → **5a** was observed.[23,24] The energies gained upon the hydration of $GlnNa^+(H_2O)_n$, $n = 0 \rightarrow 1$ (12.2 kcal/mol) and $n = 1 \rightarrow 2$ (10.3 kcal/mol) are probably not sufficient to overcome the isomerization barriers for **4** ↔ **4a** and **5** ↔ **5a**. Since our measured water binding energies are in good agreement with those experimental and calculated[23,24] for the nonzwitterionic forms of $GlnNa^+(H_2O)_{n=1,2}$, one may expect that the NOO-coordinated nonzwitterionic structures are involved in the (0,1) and (1,2) hydration equilibria of these complexes in the present experiments.

For the hydrates of $MetNa^+$ and $PheNa^+$, to our knowledge neither experimental nor computational data are available for comparison with the present study. In the $MetNa^+$ case, the lowest-energy structure is likely to be similar to that of $CysNa^+$,[6,12,16] which involves tridentate binding between the nitrogen, the carbonyl oxygen and the side-chain heteroatom (NOS coordination). The most favorable conformation found[8,9,19] for the $PheNa^+$ complex involves interaction of Na^+ to the nitrogen, the carbonyl oxygen and the aromatic ring (NO/ring coordination). As in the $GlyNa^+$, $ValNa^+$, and $GlnNa^+$ cases, the first water molecule is expected to bind directly to the sodium ion in these complexes without changes in metal-ion coordination. However, it is not clear whether the addition of a second water molecule to the singly hydrated complexes changes the sodium ion and water molecule to OO-ccordination. This process requires substantial structural rearrangement.

For the $ProNa^+$ system, both experimental and theoretical studies[13,18,33] show that the metal ion is typically OO-coordinated in the zwitterionic form, **6**. This complex is found to be 5−6 kcal/mol lower in energy than the nonzwitterionic form.[18] As shown in Table 1 and Figure 4a, the $-\Delta H_n^\circ$ values for $ProNa^+(H_2O)_n$, decrease with n. This effect can be attributed to the decreasing positive charge on Na^+ and increasing repulsion between the H_2O ligands with successive addition to $ProNa^+$. The $-\Delta H_n^\circ$ values decrease monotonically with $n = 1-3$ and marked drop is observed at $n = 4$; the $-\Delta S_n^\circ$ values show an increase up to $n = 3$ and a falloff at $n = 4$. It is worth noting that similar behavior of both $-\Delta H_n^\circ$ and $-\Delta S_n^\circ$ values vs n is observed for the $Na^+(H_2O)_{n=3-6}$ system (Figure 4). The "smaller" values of $-\Delta H_n^\circ$ for $ProNa^+(H_2O)_{n=1-4}$ compared

SCHEME 1

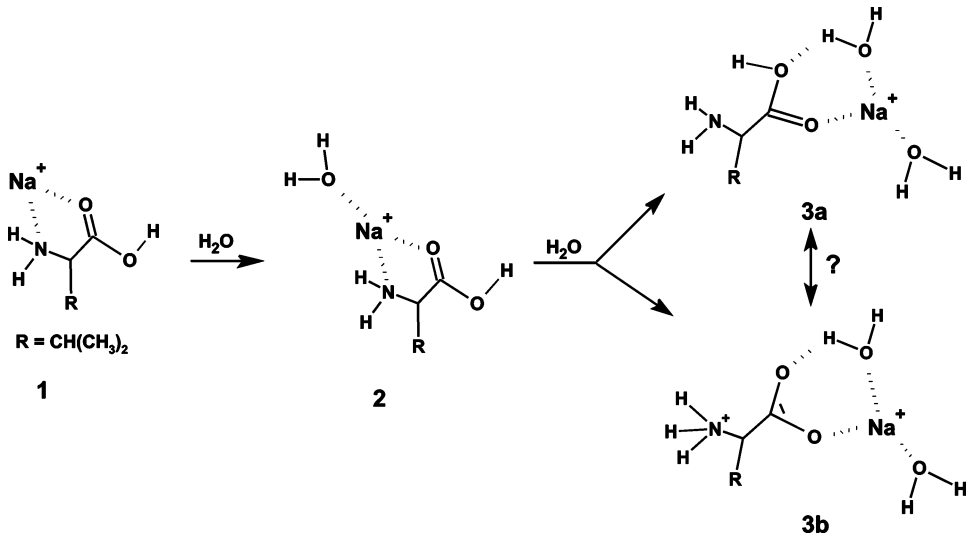

SCHEME 2

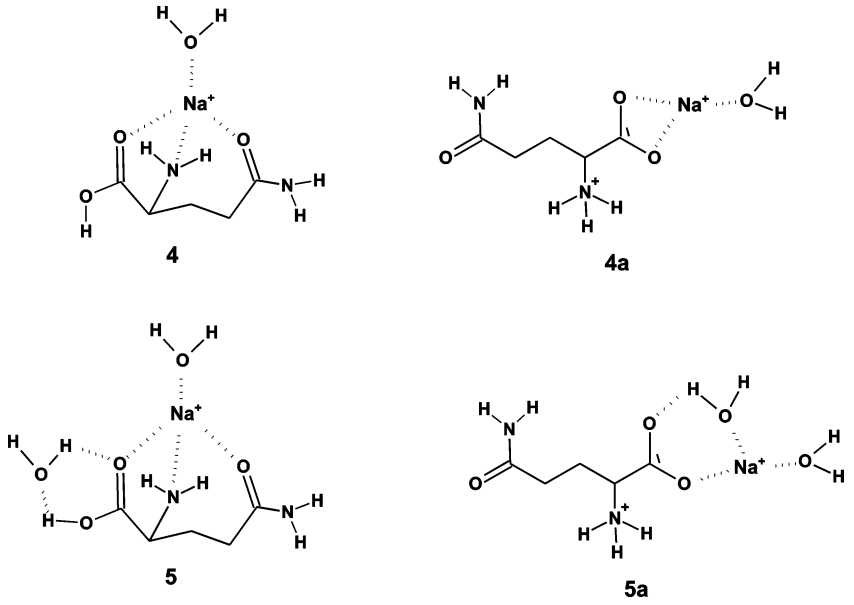

to those of $Na^+(H_2O)_{n=3-6}$ suggest that the solvation effect on a shift of the charge density from Na^+ toward proline is slightly larger than that of two water molecules. A gradual increase in the $-\Delta S_n^\circ$ values with n in the case of $ProNa^+(H_2O)_{n=1-3}$, Figure 4b, suggests that the first three water molecules experience quite isotropic potential around the Na^+ ion and thus they are separated from each other in order to minimize the exchange repulsion and to maximize the freedom of motion with the increase of n up to $n = 3$. All these results imply that the first three H_2O molecules are attached directly to the Na^+ in the $ProNa^+(H_2O)_n$ complex, **7**, while with $n = 4$ there appears an entropy barrier due to crowding around the Na^+ ion. The sudden decrease in both $-\Delta H_n^\circ$ and $-\Delta S_n^\circ$ values with $n = 3 \rightarrow 4$ suggests the switch of the attacking site by the fourth H_2O molecule. It is likely that it binds to the $-NH_2^+$ charge center to form a structure such as **7**. These results are in line with the computational characterization by Armentrout and co-workers[27] of the low-energy conformers of $ProNa^+(H_2O)_{n=1-4}$ complexes. In particular, their calculations predict that in the zwitterionic lowest-energy structure of $ProNa^+(H_2O)_4$, Na^+ is coordinated with its first solvent shell formed by the carbonyl oxygen and the other three water molecules, and the fourth water molecule hydrogen bonds to $-NH_2^+$.

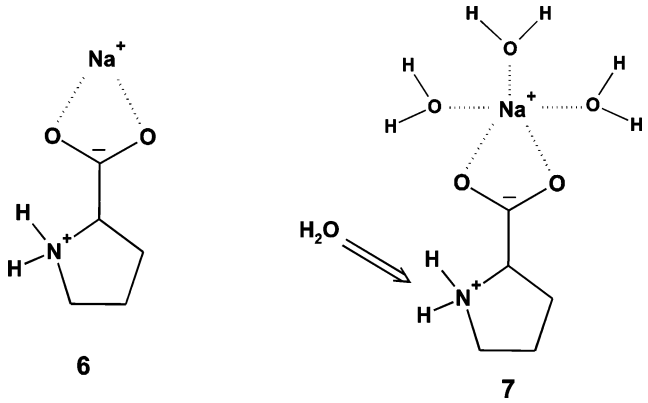

As mentioned above, there are considerable discrepancies in the hydration energies for $ProNa^+(H_2O)_n$ with $n = 3$ and 4 obtained here and the values measured by Armentrout and co-workers[27] with the TCID method (Table 1). The experimental

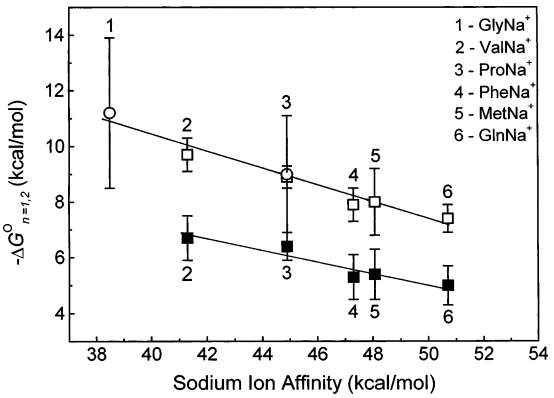

Figure 5. Plot of the hydration free energies, $-\Delta G^{\circ}_{n=1,2}$, at 298 K for the first (open symbols) and second (solid symbols) water molecule adding to $AANa^+$ versus corresponding sodium ion affinity of amino acids (AA's). The $-\Delta G^{\circ}_{n=1,2}$ values for $ValNa^+$, $ProNa^+$, $PheNa^+$, $MetNa^+$, and $GlnNa^+$, present work (□,■); $GlyNa^+$ and $ProNa^+$, refs 26 and 27 (○). For Gly, Val, Phe, and Gln, the sodium ion affinity values are taken from ref 15; for Pro and Met, from refs 27 and 34.

$-\Delta H^{\circ}_n$ values determined[27] for the $n = 3$ and 4 complexes are lower than the present results and the calculated[27] ones. A possible cause for the "lower" $-\Delta H^{\circ}_n$ values in the TCID experiments[27] could be incomplete thermalization of the complexes undergoing collision-induced dissociation (CID) in a gas collision cell.

On the other hand, in the present experiments, due to the adiabatic cooling, the ligand addition to the cluster ions can occur during transfer through the ion exit slit (ES, Figure 1) and in the vacuum region immediately outside the ion exit slit. This effect would result in overestimated $-\Delta H^{\circ}_n$ values. Conversely, collision-induced dissociation in the vacuum region outside the ion exit slit can induce the destruction of the larger cluster ions, leading to anomalous (nonlinear) course of the van't Hoff plot. The cross sections of such dissociations are expected to increase as n increases because the clusters get larger and the binding energies weaker. The narrow ion exit slit (15 μm $\times$ 3 mm) with sharp edges used in the present apparatus considerably minimizes the collisions between ions and water molecules during the expansion of the gas through the ion exit slit. It should be pointed out that the collisions of the ions are predominantly with the bath gas whose number density is 2 orders of magnitude higher than that of water. The fact that no bending in the van't Hoff plots was observed (Figure 3) suggests that the effect of CID was negligible under the present experiments and argues for the idea that the growth of the cluster ions outside the reaction chamber due to adiabatic cooling could be also negligible.

The present results and others[23] indicate that the side chains significantly affect water binding energies to the $AANa^+$ complexes. The plot of the hydration free energies ($-\Delta G^{\circ}_{n=1,2}$) for the first and second water molecule added to $AANa^+$ versus the corresponding Na^+ affinities of AA's is shown in Figure 5. With the exception of Pro and Met, the Na^+ affinity values reported by Wesdemiotis et al.[15] were used for this figure. For Pro, we take the value of 44.9 kcal/mol obtained by Moision and Armentrout,[18] which lies between the values of 41.8 kcal/mol[16] and 46.8 kcal/mol[15] from other laboratories. For Met, Armentrout and co-workers[34] obtained a value of 48.1 kcal/mol. As is evident from Figure 5, a fair linear correlation exists between the $-\Delta G^{\circ}_1$ and $-\Delta G^{\circ}_2$ values, and the respective Na^+ affinities of AA's. The correlation coefficients for the first and second waters are 0.98 and 0.95, respectively. Assuming that the first water binds directly to the Na^+ ion of $AANa^+$ systems, this effect can be attributed to the positive charge delocalization from Na^+ to AA, resulting in a lower electrostatic interaction between Na^+ and H_2O. The charge density on the Na^+ ion is expected to decrease as the Na^+ affinity of AA increases. The relationship in Figure 5 suggests that the side chain of AA is a dominant factor determining the magnitude of the residual charge density on Na^+ in $AANa^+$ complexes. The same trends in the correlation, Figure 5, obtained for the first and second waters led to the suggestion that both water molecules interact directly with the Na^+ ion in the systems studied.

Conclusion

In the present work, the gas-phase sequential hydration of several sodiated amino acids (glutamine, methionine, phenylalanine, proline and valine) have been investigated by pulsed high-pressure mass spectrometry with electrospray ionization. Water binding energies ($-\Delta H^{\circ}_n$) determined herein are of the order of 8−16 kcal/mol. Stepwise addition of water molecules leads to decrease in the relative stability of the hydrated complexes studied. These trends are attributed to the decreasing positive charge on the sodium ion and increasing repulsion between the water ligands with successive addition to the complex. The present results from HPMS experiments are compared to previous experimental measurements of the analogous systems studied by BIRD and TCID methods.

Acknowledgment. This study was supported by Grant No. 3T09A02728 from the Ministry of Science and Higher Education (Poland). Professor P. B. Armentrout is acknowledged for providing a preprint of ref 27 and for communicating the results (ref 34) of his group prior to publication.

References and Notes

(1) Lippard, S. J.; Berg, J. M. *Principles of Bioinorganic Chemistry*; University Science Books: Mill Valley, CA 1994.
(2) Stryer, L., Ed. In *Biochemistry*; Freeman, W. H.: New York, 1995; Chapter 12.
(3) Hughes, M. N., Ed. *The Inorganic Chemistry of Biological Processes* 2nd ed.; John Wiley & Sons: Chichester, U.K., 1981.
(4) Bojesen, G.; Breindahl, T.; Andersen, U. N. *Org. Mass Spectrom.* **1993**, *28*, 1448−1452.
(5) Klassen, R. G.; Anderson, S. G.; Blades, A. T.; Kebarle, P. *J. Phys. Chem.* **1996**, *100*, 14218−14223.
(6) Hoyau, S.; Norrman, K.; McMahon, T. B; Ohanessian, G. *J. Am. Chem. Soc.* **1999**, *121*, 8864−8875.
(7) Jockusch, R. A.; Price, W. D.; Williams, E. R. *J. Phys. Chem. A* **1999**, *103*, 9266−9274.
(8) Dunbar, R. C. *J. Phys. Chem. A* **2000**, *104*, 8067−8074.
(9) Ryzhov, V.; Dunbar, R. C.; Cerda, B.; Wesdemiotis, C. *J. Am. Soc. Mass Spectrom.* **2000**, *11*, 1037−1046.
(10) Marino, T.; Russo, N.; Toscano, M. *Inorg. Chem.* **2001**, *40*, 6439−6443.
(11) Moision, R. M.; Armentrout, P. B. *J. Phys. Chem. A* **2002**, *106*, 10350−10362.
(12) Talley, J. M.; Cerda, B. A.; Ohanessian, G. Wesdemiotis, C. *Chem. Eur. J.* **2002**, *8*, 1377−1388.
(13) Marino, T.; Russo, N.; Toscano, M. *J. Phys. Chem. B* **2003**, *107*, 2588−2594.
(14) Lau, J. K.-C; Wong, C. H. S.; Ng, P. S.; Siu, F. M.; Ma, N. L.; Tsang, C. W. *Chem. Eur. J.* **2003**, *9*,3383−3396.
(15) Kish, M. M.; Ohanessian, G.; Wesdemiotis, C. *Int. J. Mass Spectrom.* **2003**, *227*, 509−524.
(16) Gapeev, A.; Dunbar, R. C. *Int. J. Mass Spectrom.* **2003**, *228*, 825−839.
(17) Moision, R. M.; Armentrout, P. B. *Phys. Chem. Chem. Phys.* **2004**, *6*, 2588−2599.
(18) Moision, R. M.; Armentrout, P. B. *J. Phys. Chem. A* **2006**, *110*, 3933−3946.
(19) Ruan, C.; Rodgers, M. T. *J Am. Chem. Soc.* **2004**, *126*, 14600−1410.

(20) Jockusch, R. A.; Lemoff, A. S.; Williams, E. R. *J. Phys. Chem. A* **2001**, *105*, 10929−10942.
(21) Lemoff, A. S.; Williams, E. R. *J. Am. Soc. Mass Spectrom.* **2004**, *15*, 1014−1024.
(22) Kamariotis, A.; Boyarkin, O. V.; Mercier, S. R.; Beck, R. D.; Bush, M. F.; Williams, E. R.; Rizzo, T. R. *J. Am. Chem. Soc.* **2006**, *128*, 905−916.
(23) Lemoff, A. S.; Bush, M. F.; Wu, C.-C.; Williams, E. R. *J. Am. Chem. Soc.* **2005**, *127*, 10276−10286.
(24) Lemoff, A. S.; Wu, C.-C.; Bush, M. F.; Williams, E. R. *J. Phys. Chem. A* **2006**, *110*, 3662−3669.
(25) Lemoff, A. S.; Bush, M. F.; Williams, E. R. *J. Phys. Chem. A* **2005**, *109*, 1903−1910.
(26) Ye, S. J.; Moision, R. M.; Armentrout, P. B. *Int. J. Mass Spectrom.* **2005**, *240*, 233−248.
(27) Ye, S. J.; Moision, R. M.; Armentrout, P. B. *Int. J. Mass Spectrom.* **2006**, *253*, 288−304.
(28) Wincel, H. *Int. J. Mass Spectrom.* **2006**, *251*, 23−31.
(29) Lemoff, A. S.; Bush, M. F.; Williams, E. R. *J. Am. Chem. Soc.* **2003**, *125*, 13576−13584.
(30) Džidić, I.; Kebarle, P. *J. Phys. Chem.* **1970**, *74*, 1466−1474.
(31) Rožman, M.; Bertoša, B.; Klasinc, L.; Srzič, D. *J. Am. Soc. Mass Spectrom.* **2006**, *17*, 29−36.
(32) Jockusch, R. A.; Lemoff, A. S.; Williams, E. R. *J. Am. Chem. Soc.* **2001**, *123*, 12255−12265.
(33) Kapota, C.; Lemaire, J.; Mãitre, P.; Ohanessian, G. *J. Am. Chem. Soc.* **2004**, *126*, 1836−1842.
(34) Gabriel, A.; Moision, R. M.; Armentrout, P. B. Work in progress.